available at www.sciencedirect.com

www.elsevier.com/locate/brainres

BRAIN RESEARCH

Research Report

Adaptive rescaling of central sensorimotor signals is preserved after unilateral vestibular damage

Raquel Heskin-Sweezie[a,b], *Karl Farrow*[a,b], *Dianne M. Broussard*[a,b,c,*]

[a]*Toronto Western Research Institute, University Health Network, Canada*
[b]*Department of Physiology, University of Toronto, Canada*
[c]*Division of Neurology, Department of Medicine, University of Toronto, Canada*

ARTICLE INFO

Article history:
Accepted 18 January 2007
Available online 1 February 2007

Keywords:
Vestibular
Oculomotor
Rescaling
Adaptation

ABSTRACT

Adaptive rescaling is a widespread phenomenon that dynamically adjusts the input–output relationship of a sensory system in response to changes in the ambient stimulus conditions. Rescaling has been described in the central vestibular neurons of normal cats. After recovery from unilateral vestibular damage, the vestibulo-ocular reflex (VOR) remains nonlinear for rotation toward the damaged side. Therefore, rescaling in the VOR pathway may be especially important after damage. Here, we demonstrate that central vestibular neurons adjust their input–output relationships depending on the input velocity range, suggesting that adaptive rescaling is preserved after vestibular damage and can contribute to the performance of the VOR. We recorded from isolated vestibular neurons in alert cats that had recovered from unilateral vestibular damage. The peak velocity of 1-Hz sinusoidal rotation was varied from 10 to 120°/s and the sensitivities and dynamic ranges of vestibular neurons were measured. Most neuronal responses showed significant nonlinearities even at the lowest peak velocity that we tested. Significant rescaling was seen in the responses of neurons both ipsilateral and contralateral to chronic unilateral damage. On the average, when the peak rotational velocity increased by a factor of 8, the average sensitivity to rotation decreased by roughly a factor of 2. Rescaling did not depend on eye movement signals. Our results suggest that the dynamic ranges of central neurons are extended by rescaling and that, after vestibular damage, adaptive rescaling may act to reduce nonlinearities in the response of the VOR to rotation at high speeds.

1. Introduction

In normal individuals, the vestibulo-ocular reflex (VOR) stabilizes gaze during head rotation over a wide range of velocities (Maioli et al., 1983; Paige, 1983a). After unilateral labyrinthectomy (UL) or unilateral plugging of the semicircular canals, compensation occurs, but the range of velocities over which the VOR can stabilize gaze remains subnormal (Maioli et al., 1983; Fetter and Zee, 1988; Paige, 1983b; Lasker et al., 1999, 2000). This restriction on the compensated VOR may be due to the limited linear ranges of central vestibular neurons. Because of the rapid and direct reflex output of the VOR, it is desirable that vestibular sensory signals should provide linear functions that can be used as motor commands. However,

* *Corresponding author*. MP12-318, Toronto Western Hospital, 399 Bathurst St., Toronto, Ontario M5T 2S8, Canada. Fax: +1 416 603 5745.
E-mail address: dianne@uhnres.utoronto.ca (D.M. Broussard).

Abbreviations: EM, eye movement; MSE, mean square error; RI, rescaling index; $SD_{H=0}$, zero-velocity spike density; s.e.m., standard error of the mean; UVD, unilateral vestibular damage; UL, unilateral labyrinthectomy; V-only, vestibular-only

0006-8993/$ – see front matter © 2007 Elsevier B.V. All rights reserved.
doi:10.1016/j.brainres.2007.01.104

many secondary vestibular neurons display cutoff responses (i.e., are silenced during rotation in their off-directions), even at low speeds (Melvill Jones and Milsum, 1970; Newlands and Perachio, 1990a; Escudero et al., 1992; Chen-Huang and McCrea, 1999; Broussard et al., 2004). In awake cats, most central vestibular neurons consistently have asymmetric responses to sinusoidal rotation (Broussard et al., 2004). Primary afferents from the semicircular canal endorgans also are not purely linear in their response characteristics, and irregularly-firing afferents can be silenced during contralateral rotation (Dickman and Correia, 1989; Hullar et al., 2005).

In spite of the nonlinear responses of its neurons, the normal VOR can generate an overall linear response, presumably because it is based on inputs from the two labyrinths which complement each other. But after unilateral labyrinthectomy, neurectomy or plugging of the horizontal canal, the head velocity signal arising from the damaged side is lost, and the VOR's response has a reduced linear range (Maioli et al., 1983; Paige, 1983b; Fetter and Zee, 1988; Tusa et al., 1996; Foster et al., 1997; Lasker et al., 2000). Thus after unilateral vestibular damage (UVD), the VOR begins to express some of the nonlinear features of its neurons. A mechanism for extension of the dynamic ranges of neuronal responses might therefore improve gaze stability after UVD.

Adaptive rescaling refers to an adjustment in the sensitivities of sensory neurons that accompanies a change in the expected dynamic range of the sensory signal and increases the efficiency of coding (Brenner et al., 2000). Flexible sensitivities, adjusted to the expected range of sensory inputs, can optimize information transmission by neurons (McLaughlin, 1967). During high-amplitude inputs, sensitivity is minimized so that the dynamic ranges of neurons are exceeded less often; this would be especially useful in the vestibular system because of the requirement for linearity. During small inputs, sensitivity is maximized, improving the accuracy of coding. Most adaptation in sensory systems is adaptive rescaling, rather than an inability of the receptor to respond to continuing stimuli. One exception is the adaptation to ongoing rotation at a constant velocity by the vestibular system, which we will call peripheral adaptation and which is a consequence of hydrodynamics and of peripheral inhibition (Rabbitt et al., 2005). In addition to peripheral adaptation, central vestibular neurons demonstrate adaptive rescaling. When the peak velocity of sinusoidal rotation is increased, central neurons in normal cats reduce their sensitivities (Melvill Jones and Milsum, 1970). In this report, we will describe adaptive rescaling after recovery from unilateral vestibular damage.

2. Results

We recorded the responses of 52 isolated cells in the medial and ventral lateral vestibular nuclei of 3 cats, during rotation at peak velocities of 10–80°/s; a subset of neurons were also tested at 120°/s. Neuronal responses were recorded under two different chronic lesion conditions, a unilateral labyrinthectomy (UL) and a unilateral horizontal semicircular canal plug. All of the cells reported here were tested at 10, 20, 40 and 80°/s peak velocities. Although some of the final samples were quite small, it was nevertheless clear that rescaling was not exclusive for a particular lesion type or for either side of the brainstem with respect to the lesion.

Cells were classified according to the polarity of their responses as types I, II or III (see Experimental procedure). The breakdown of our sample according to lesion type, side and response type is shown in Table 1. All neurons had non-zero resting discharge rates. In the ipsilesional vestibular nuclei, the largest subgroup of cells responding to rotation showed type II responses (54%). On the contralesional side, only 17% were type II and 75% were type I. The prevalence of type II responses ipsilateral to UVD was expected based on earlier studies (Shimazu and Precht, 1966; Smith and Curthoys, 1988b; Newlands and Perachio, 1990a,b). The observation that type I neurons were prevalent contralateral to UVD also agreed with earlier reports (Shimazu and Precht, 1966; Smith and Curthoys, 1988a; Newlands and Perachio, 1990a,b).

Neuronal sensitivities to rotation were measured as illustrated in Fig. 1. Spike density was plotted against head velocity; any phase lead or lag was removed. To determine the linear range for sensitivity measurements, a best fit of two lines was used (Fig. 1). If the slopes were significantly different, a breakpoint was defined as the head velocity at the intersection of the fitted lines; otherwise the response was said to be linear (Fig. 1C). For cutoff responses, the sensitivity was the slope of the response function above the breakpoint (arrow in Fig. 1) and for saturation-type responses, the sensitivity was the slope below the breakpoint. Further details are given under Experimental procedure.

Table 1 – Neuronal types and lesion conditions

Side	Lesion	Cat(s)	Cell type	Sample sizes	Total for type (*n*)	Total for side	% of type
Ipsi	UL	O	I	4	–	–	–
Ipsi	UL	O	II	12	–	–	–
Ipsi	UL	O	III	5	–	–	–
Ipsi	CP	J	I	1	–	–	–
Ipsi	CP	J	II	1	–	–	–
Ipsi	CP	J	III	1	–	–	–
Ipsi	**Either**	**O, J**	**I**	–	**5**	**24**	**21**
Ipsi	**Either**	**O, J**	**II**	–	**13**	**24**	**54**
Ipsi	**Either**	**O, J**	**III**	–	**6**	**24**	**25**
Contra	UL	O	I	1	–	–	–
Contra	UL	O	II	1	–	–	–
Contra	UL	O	III	0	–	–	–
Contra	CP	C	I	20	–	–	–
Contra	CP	C	II	4	–	–	–
Contra	CP	C	III	2	–	–	–
Contra	**Either**	**O, C**	**I**	–	**21**	**28**	**75**
Contra	**Either**	**O, C**	**II**	–	**5**	**28**	**17**
Contra	**Either**	**O, C**	**III**	–	**2**	**28**	**7**

This table shows the samples, subdivided according to neuronal type, that were obtained from each side of the brain in each cat. The rows in boldface type summarize the samples of cells from each side of the brain.

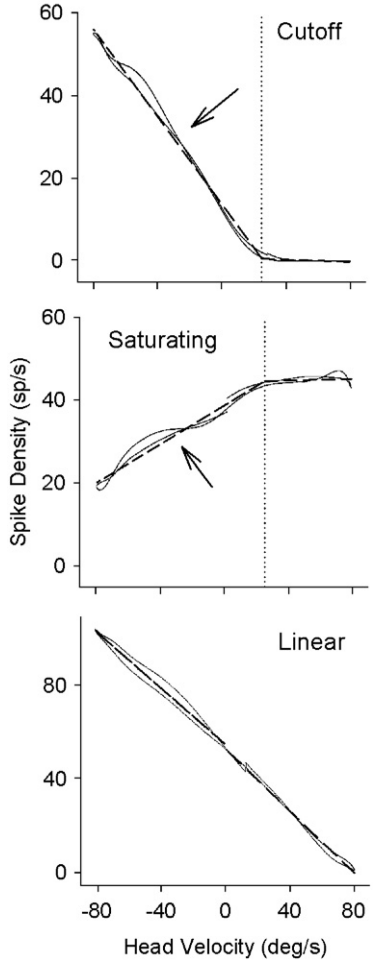

Fig. 1 – Sample responses to rotation. Positive values are rightward angular velocity in all figures. Spike density is plotted as a function of velocity (thin lines); spike density has been shifted in time to remove phase differences. Heavy dotted lines are linear fits to the data. For the *cutoff* and *saturating* responses, the breakpoints between the two linear fits (vertical dotted lines) were identified with significant differences between the slopes of the lines on either side. For the *linear* response, there was no significant difference. Sensitivity was defined for cutoff responses as the slope of the line that included rotation in the "on" direction (arrow), for saturating responses as the slope in the "off" direction (arrow) and for linear cells, as the average slope of the two lines. Data are from the ipsilesional side in cat O (cutoff, saturating) and the contralesional side in cat C (linear).

Relatively few cells gave consistently linear responses across the range of velocities that were tested. The numbers of cells of the two most prevalent response types (types I and II) that showed linear, saturating and cutoff responses at the highest velocity tested are given in Table 2. On the undamaged side, the majority of type I neurons showed cutoff responses. On the ipsilesional side, cutoff responses clearly prevailed among type II neurons. The other two groups were too small for a conclusive outcome, but we can observe that all three response types occurred in each group of cells.

2.1. *Adaptive rescaling of neuronal responses*

The majority of vestibular neurons reduced their sensitivities to rotation as the peak angular velocity was increased. Examples of rescaling in the input–output functions of typical ipsi- and contralesional vestibular neurons are shown in Figs. 2A and B, respectively. The linear part of the input–output function for each cell, as we defined it (see Experimental procedure), showed a decrease in slope with increasing peak velocity. In cells that demonstrated a cutoff pattern, like the examples in Fig. 2, lowering the sensitivity to rotation increased the dynamic range of signaling at the higher rotation velocities.

To quantify rescaling for each cell, we defined a rescaling index (RI) as the ratio of the sensitivities at 10 and 80°/s. In Figs. 2C–D, RI is plotted for our sample of cells as a function of each cell's sensitivity to head velocity when measured at a peak velocity of 10°/s. Ipsilesional and contralesional cells, and type I and type II responses, are represented by different symbols. Most of the sample fell between an RI of 1.0 (dotted line), indicating no rescaling, and an RI of 4.0, with an overall mean of 1.82. A few cells had an RI less than 1, and the majority of these also exhibited very low sensitivities to rotation (<0.25 sp/s per degree/s). Overall, an 8-fold increase in stimulus velocity coincided with an approximately 2-fold decrease in sensitivity. There was no significant difference in RI between ipsilesional and contralesional neurons ($P>0.5$, Student's *t*-test). Over the entire sample, RI was not correlated with sensitivity.

Fig. 3 summarizes the relationship between the sensitivity of the linear region of each cell's input–output function and the peak rotation velocity, for four groups of cells. For each of the four groups (also shown in Table 2), sensitivity was averaged across cells for the 10–80°/s range of peak velocities (heavy lines) and also across the subset of cells that were tested at 120°/s (symbols and lines). As rotation velocity was increased, sensitivity to rotation consistently and systematically decreased for all four groups. Rescaling was most pronounced in

Table 2 – Input–output function types

Side	Lesion	Cat (s)	Cell type	Input–output type	Number of I–O type	Total of cell type	% of I–O type
Ipsi	Either	O, J	I	Cutoff	1	5	20
Ipsi	Either	O, J	I	Sat.	3	5	60
Ipsi	Either	O, J	I	Linear	1	5	20
Ipsi	Either	O, J	II	Cutoff	10	13	77
Ipsi	Either	O, J	II	Sat.	1	13	8
Ipsi	Either	O, J	II	Linear	2	13	15
Contra	Either	O, C	I	Cutoff	14	21	67
Contra	Either	O, C	I	Sat.	3	21	14
Contra	Either	O, C	I	Linear	4	21	19
Contra	Either	O, C	II	Cutoff	2	5	40
Contra	Either	O, C	II	Sat.	1	5	20
Contra	Either	O, C	II	Linear	2	5	40

This table shows the number of neurons of types I and II that responded with cutoff, saturating or linear input–output functions, for both the ipsilesional and contralesional sides. Type III neurons did not fit any of the input–output types (as defined in Experimental procedures).

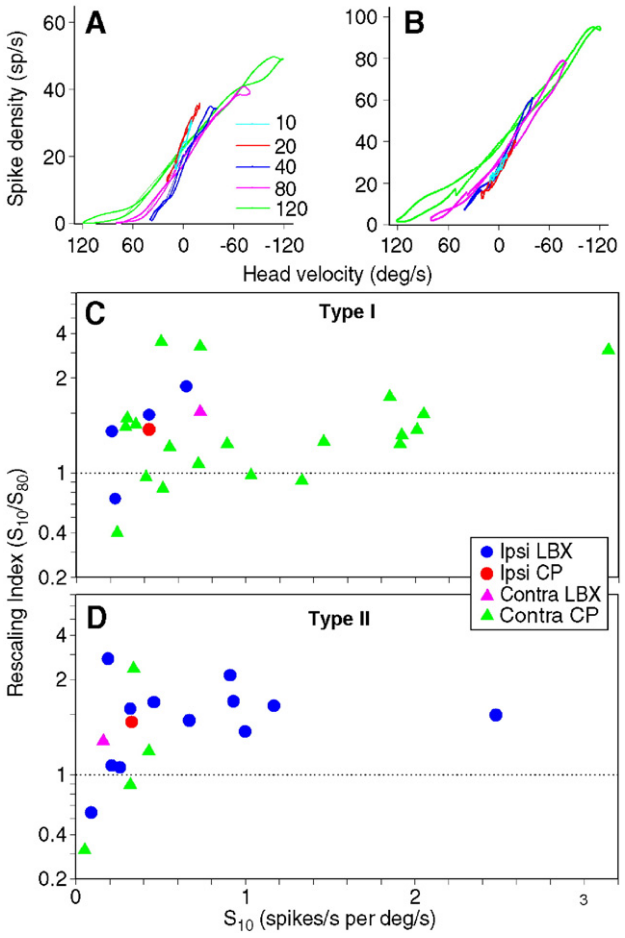

Fig. 2 – Adaptive rescaling occurred under all tested conditions and was not specific for the type of lesion, response type or side of recording. (A,B) Examples of adaptive rescaling. Averaged spike densities are plotted as a function of the head velocity during a full cycle of rotation. Different colors represent different peak velocities according to the legend. (A) A vestibular neuron ipsilateral to the UL. (B) A vestibular neuron contralateral to a horizontal canal plug. As peak velocity increased, neuronal sensitivities to rotation decreased. The cells shown in A and B were both located in the medial vestibular nucleus. (C) Rescaling index (RI) versus sensitivity for all type I neurons in the sample. Sensitivity was measured at 10°/s peak head velocity. Different symbols indicate the side with respect to the lesion and the lesion type. D: RI versus sensitivity for type II neurons.

the groups that were most sensitive to rotation. On the ipsilesional side, type II cells showed a significant reduction in sensitivity when the peak velocity was increased to 80°/s (Student's *t*-test, $P<0.01$, $n=13$). The ipsilesional type I cells, which were less sensitive as well as less abundant, also appeared to rescale but the change was not significant.

The sample of type I cells on the contralesional side, which were more sensitive than their type II counterparts, changed their sensitivities significantly when peak velocity was increased to 80°/s ($P<0.01$, $n=21$). Type II neurons on the contralesional side ($n=5$) showed a less uniform trend in sensitivity. It should be noted that, for the contralesional type I neurons, the first velocity tested was 20°/s, but the sensitivity at 20°/s was still lower than it was at 10°/s. For all four groups of cells, sensitivity appeared to be related to peak velocity by a power law.

2.2. *The phase of rescaled responses*

We measured phase differences between spike density and head velocity by optimizing the linear fits. Spike density led head velocity by a small amount at all velocities. Phase leads increased with increasing peak velocity for all four of the groups of Fig. 3 but in most cases, the increase was not significant. For contralesional type I cells, there was a significant increase in the phase lead as peak velocity increased from 10 to 20°/s (Student's *t*-test, $P<0.01$). The different groups of cells also showed minor differences in their mean response phases; phases were significantly different between ipsilesional type I and type II cells ($P<0.01$). None of the other groups was significantly different from one another.

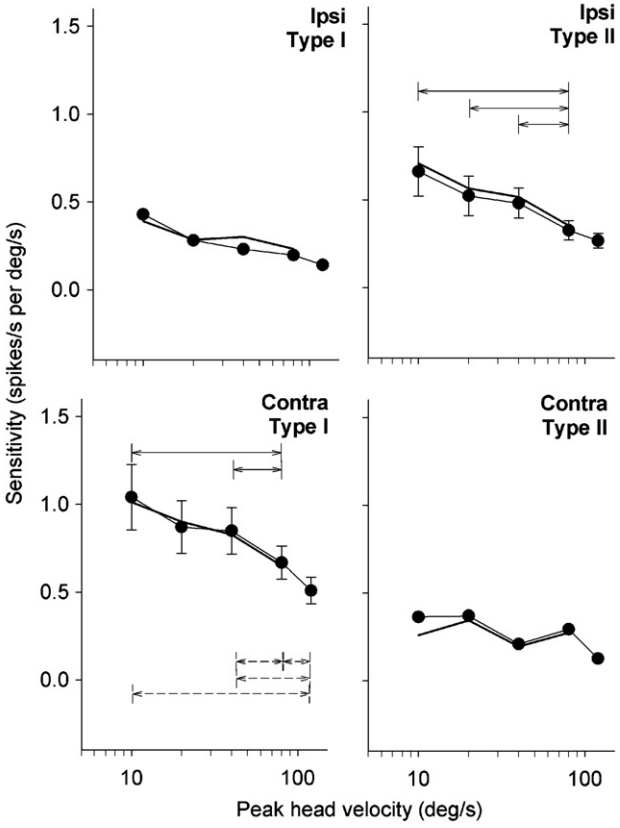

Fig. 3 – Changes in sensitivity as a function of peak head velocity. For the four major groups of cells, mean sensitivities are shown for the sample of cells that were tested at velocities up to 80°/s (solid lines) and for the subset that was tested up to 120°/s (symbols, dashed lines). For type I cells ipsilateral to the lesion, $n=5$ up to 80°/s and $n=3$ for 120°/s. For type II cells ipsilateral to the lesion, $n=13$ for 80°/s and $n=7$ for 120°/s. For type I cells contralateral to the lesion, $n=21$ for 80°/s and $n=18$ for 120°/s. For type II cells contralateral to the lesion, $n=5$ for 80°/s and $n=3$ for 120°/s. In this and all figures, error bars are standard errors of the mean (s.e.m.). The pairs of samples for which a paired Student's *t*-test indicated $P<0.01$ are indicated by the solid arrows for the full sample, and the dashed arrows for the 120°/s subset.

Overall, a slight increase in phase lead, not significant in most groups of cells, was seen with rescaling to higher velocities.

2.3. *Lack of rescaling with changes in rotation frequency*

The phase of the neuronal responses indicated that predominantly velocity signals were present. If rescaling were associated primarily with an acceleration signal carried by secondary neurons, rescaling should occur when rotation frequency was increased with no change in velocity. We tested a subset of our sample (11 contralesional and 13 ipsilesional cells) at frequencies from 1 to 8 Hz and peak velocities of 10°/s (data not shown). We saw no significant changes in sensitivity or phase with the 8-fold increase in peak acceleration, suggesting that acceleration signals were not responsible for rescaling.

2.4. *Eye movement sensitivity and rescaling*

Motor command signals, which are present on many vestibular neurons, could contribute to rescaling. To address this possibility, we compared rescaling in eye movement (EM) and vestibular-only (V-only) cells. Fig. 4 shows the sample of cells that were tested for eye position sensitivity, divided into EM and V-only cells. Fewer than half ($n=17$) had discharge rates that depended on eye position with a sensitivity of more than 0.5 spikes/s per degree and were therefore considered EM cells. The remainder ($n=19$) were considered V-only neurons. Both EM and V-only neurons showed evidence of rescaling. There was no difference in RI between EM and V-only cells ($P>0.5$, Student's t-test). There was also no correlation between eye position sensitivity and RI. This negative finding suggested that rescaling may be either a property of sensory inputs or an intrinsic property of the neurons.

2.5. *Changes in zero-velocity spike density ($SD_{H=0}$)*

Adaptive rescaling was accompanied by changes in our estimate of the resting discharge rate, $SD_{H=0}$. Fig. 5 illustrates the effect of peak velocity on $SD_{H=0}$ for the same cells that were shown in Fig. 3. For type I neurons on both the ipsilesional and contralesional sides, $SD_{H=0}$ increased significantly with peak rotation velocity ($P<0.01$, Student's t-test). The change in $SD_{H=0}$ with peak velocity was not significant for type II cells on either side of the brainstem.

For the ipsilesional cells that were tested at 120°/s, we measured spike densities at rest immediately after the end of the testing protocol (open squares in Fig. 5) to rule out artifacts such as increasing pressure exerted by the recording electrode. The resting rate was not significantly different ($P>0.1$, paired t-test) at the end compared with the beginning of the experiment (filled squares). The post-rotation increase for ipsilesional type I neurons (indicated by the arrow) was due to a change in one cell and was not statistically significant. For the contralesional cells, however, we cannot rule out a contribution of recording artifacts to the observed changes in $SD_{H=0}$.

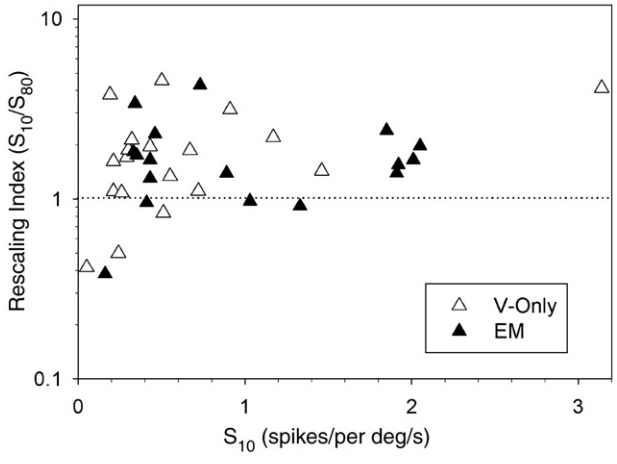

Fig. 4 – Cells that were tested for eye position sensitivity are classified according to side of recording, response polarity and eye position sensitivity. Rescaling occurred within each subgroup. No difference was seen overall between EM and V-only cells (see text for details).

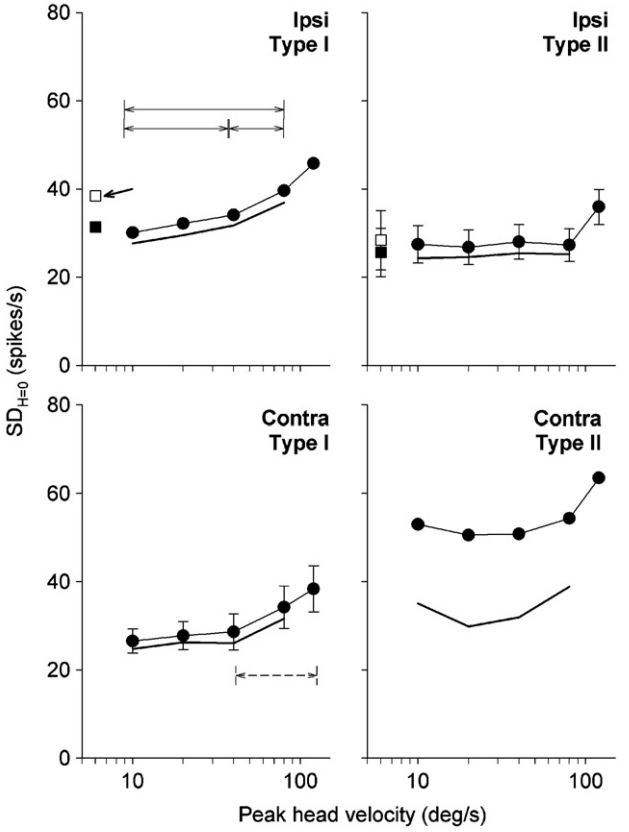

Fig. 5 – Zero-velocity spike density ($SD_{H=0}$) measurements (mean ± s.e.m.). $SD_{H=0}$, a measure of resting discharge rate, increased with increasing peak head velocity. Symbols, lines, sample sizes and arrows as in Fig. 3, except that the square symbols represent resting rates that were measured before (filled squares) and after (open squares) the rotation series.

2.6. *Effect of rescaling on dynamic range*

If a neuron decreases its discharge rate in proportion to rotation velocity, rotation in the off-direction at some head velocity will silence the cell. This condition is known as cutoff and limits the dynamic range of the neuron. If we assume that

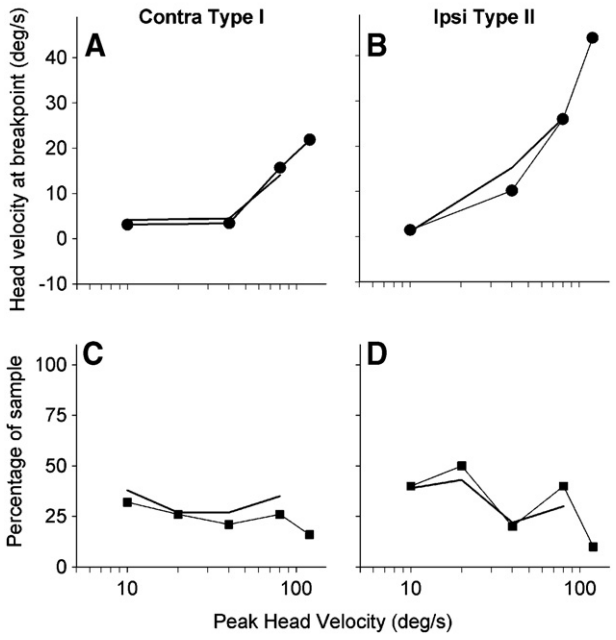

Fig. 6 – The linear ranges of central neurons. (A) Breakpoints for type I cells from the contralesional vestibular nuclei ($n=4$). (B) Breakpoint measurements (mean ± s.e.m.) for type II cells from the ipsilesional side ($n=6$). For the plots that include 120°/s, $n=3$ for both ipsilesional and contralesional sides. Only cells that showed cutoff responses with clear breakpoints at all velocities were included in A and B. (C, D) The percentage of neurons showing linear responses for each sample, as a function of head velocity.

vestibular neurons have linear input–output functions apart from cutoff, then a neuron would be expected to reach cutoff at the head rotation velocity predicted by the relationship

$$H'_{\text{cutoff}} = \text{SD}/S \quad (1)$$

where SD is the $\text{SD}_{H=0}$ and S is the sensitivity, in spikes/s per degree/s, at the velocity being tested. Either a decrease in sensitivity or an increase in $\text{SD}_{H=0}$ would be expected to increase the cutoff velocity, and therefore the dynamic range, of vestibular neurons.

Quantitatively, Eq. (1) was a poor predictor of the breakpoints in our sample of neurons. Most cells displayed significant cutoff-type nonlinearities without reaching zero spike density. Qualitatively, however, the prediction that the breakpoint should increase with peak stimulus velocity was borne out. In Fig. 6, the value of head velocity at the breakpoint is plotted as a function of peak head velocity for the cells that showed cutoff-type responses with clear breakpoints at all velocities. Only 10 cells met this criterion; all were either ipsilesional type II or contralesional type I. For the ipsilesional type II cells, the breakpoint changed significantly when peak velocity was increased to 80°/s ($P<0.01$, paired t-test, $n=6$). As a consequence, the range of velocities over which the input–output functions of these cells were linear increased with increasing head velocity. The same trend was seen in the type I contralesional cells.

Even at a peak velocity of 10°/s, fewer than 50% of neuronal responses were linear; surprisingly, this did not change much as peak velocity increased. Figs. 6C and D illustrate the percentage of linear responses at each peak velocity. No cells reached a spike density of zero, but the responses of most neurons showed significant breakpoints, either at low or high discharge rates. On the contralesional side there was no decrease in the percentage of linear responses as peak head velocity increased from 10 to 80°/s, and only a slight decrease in the percentage was seen at 120°/s. The observation that, contralateral to the lesion, the linear responses remained linear over the entire range of velocities may be due to rescaling in individual neurons. In contrast, on the ipsilesional side, the percentage of linear responses decreased from 40% at the lowest peak velocity to only 10% at the highest velocity tested.

2.7. *Time course of sensitivity*

Except for a single breakpoint, each cell's response yielded good linear fits, suggesting that sensitivity remained constant as velocity changed within each cycle of rotation and that sensitivity must change over a longer time course. We

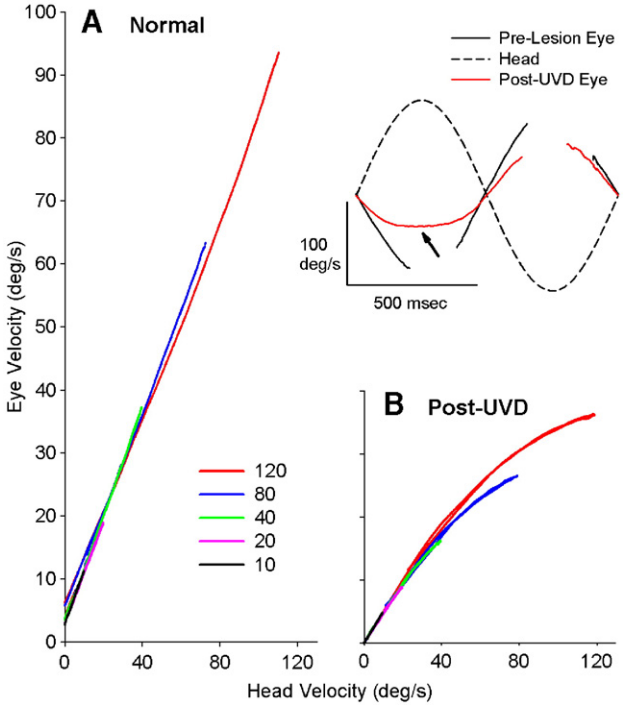

Fig. 7 – The VOR before and after UVD. The *inset* shows a full cycle of rotation at 1 Hz and the VOR's response in cat O before and after UVD, at a peak velocity of 120°/s. The dashed line is head velocity and the solid lines are eye velocity. Thirty cycles were averaged and the gaps indicate the locations of consistent quick phases. Note the saturation in the VOR for ipsilesional rotation, which is rightward in this case (arrow). (A) Slow-phase eye velocity is plotted against head velocity for the rightward half-cycle at various peak velocities (colors) before the lesion. 320 cycles were averaged for each plot, from data that were gathered across 8 days. (B) Eye velocity as a function of head velocity for the same cat after UVD. Rotation is toward the lesioned (right) side.

measured changes in sensitivity over time by dividing the records into groups or bins of 5 cycles apiece, for four cells from each of the two largest groups (type II ipsilesional and type I contralesional cells). This analysis confirmed consistent rescaling between peak velocities but did not reveal consistent changes in sensitivity between the 5-cycle bins, suggesting that rescaling was too rapid to be measured with this method.

2.8. *The significance of adaptive rescaling for VOR performance*

The velocity range of adaptive rescaling encompassed the transition from linear to nonlinear VOR performance after UVD. Fig. 7 shows the response of the VOR to 1-Hz horizontal rotation before UVD and toward the damaged side after UVD, at peak velocities between 10 and 120°/s in the cat from which the ipsilesional cells were recorded. Before the lesion (Fig. 7A), the VOR was linear at all peak velocities. When the VOR was recorded after UVD (Fig. 7B), nearly linear responses were obtained for peak velocities up to 20°/s but saturating responses were obtained at 40–120°/s. In the second cat, the results were similar to those in Fig. 7; slow-phase responses showed evidence of saturation for rotation toward the damaged side, at 40°/s and higher peak velocities (data not shown).

The VOR gain did not rescale along with neuronal sensitivities. Within the (limited) linear range of the VOR, the slope of the input–output functions in Fig. 7 did not vary with peak velocity, even though the sensitivities of central vestibular neurons clearly did change (Fig. 3).

At 80 and 120°/s the VOR showed saturating responses, which coincided with nonlinear responses in nearly all vestibular neurons on the ipsilesional side. Although there was no change in slope, the dynamic range of the VOR appeared to increase (compare 80°/s and 120°/s curves in Fig. 7).

3. Discussion

Changes in the sensitivities of central vestibular neurons, depending on the peak rotational velocity, were described in early experiments using normal cats (Melvill Jones and Milsum, 1970). Because many central vestibular neurons are also premotor neurons, in this system we can reasonably hope to understand the effect of sensory rescaling on motor commands. Nevertheless, adaptive rescaling in the VOR has not been investigated further until now. We describe adaptive rescaling in the central vestibular neurons of alert cats that have recovered from UVD and conclude that adaptive rescaling is preserved, both after UL and after canal plugging.

As in the earlier report of rescaling in decerebrate, labyrinth-intact cats (Melvill Jones and Milsum, 1970), we found changes in neuronal sensitivities by a factor of only 2, while the stimulus changed by a factor of 8 in amplitude; in other words, rescaling did not quantitatively match the dynamic range of the output to the range of input signals. However, rescaling did increase the dynamic ranges of individual cells' responses to rotation. The dynamic ranges of vestibular neurons increased over the same range of peak velocities that induced saturating responses in the post-UVD VOR. The dynamic range of eye velocities during the VOR also increased with peak velocity. A possible interpretation is that, after UVD, rescaling acts to adjust the linear range of the VOR to the expected dynamic range of head movement.

The function of rescaling can be described as a tradeoff, substituting decreased sensitivity for nonlinear responses. This tradeoff has been shown to be advantageous in the visual and auditory systems (Fairhall et al., 2001; Kim and Rieke, 2001; Schwartz and Simoncelli, 2001; Dean et al., 2005; Nagel and Doupe, 2006). Rescaling, also known as gain control or sensory adaptation, also occurs in the somatosensory (Khatri et al., 2004; Leung et al., 2005) and accessory optic (Ibbotson, 2005) systems. Rescaling in sensory systems is associated with an increase in information transmission (Brenner et al., 2000; Fairhall et al., 2001; Borst et al., 2005; Dean et al., 2005). It is complete within a few seconds of a change in the range of stimuli (Ohzawa et al., 1985; Fairhall et al., 2001; Kim and Rieke, 2001; Leung et al., 2005). In the vestibular system, rescaling can help to maintain the linear responses that are required for good gaze stabilization. Our results are consistent with a rapid adjustment in sensitivity during the first second of rotation.

3.1. *Adaptive mechanisms in the VOR*

Peripheral adaptation, motor learning and habituation all affect the gain of the VOR, but our results could not be explained by any of these known mechanisms. Of the three, only peripheral adaptation has a similar time course to adaptive rescaling. Peripheral adaptation is measured in the responses of primary afferents as a decline in the firing rate during a long period (30–60 s) of constant velocity or acceleration. The time constant of peripheral adaptation is 3.8 s in cats (Blanks et al., 1975) and it reduces the sensitivity of central vestibular neurons to rotation at frequencies below about 0.3 Hz, relative to higher frequencies (Melvill Jones and Milsum, 1971). The responses of primary afferents and central neurons to rotation at the frequency we used, 1 Hz, are not affected by peripheral adaptation (Fernandez and Goldberg, 1971; Melvill Jones and Milsum, 1971; Rabbitt et al., 2005). In general, peripheral adaptation is a feature of linear temporal dynamics and is independent of rotational velocity (Fernandez and Goldberg, 1971; Melvill Jones and Milsum, 1971; Rabbitt et al., 2005), while adaptive rescaling introduced a significant dependence of sensitivity on rotational velocity.

3.2. *Afferent diversity and adaptive rescaling*

Adaptive rescaling at the level of secondary vestibular neurons could be "inherited" from primary afferents, reflecting some process that takes place within the labyrinth. Primary afferents on the damaged side are assumed to be silenced after UL, but rescaling in primary afferents on the intact side could bring about rescaling in secondary neurons on both sides. An attractive candidate for a peripheral rescaling process is the integration of signals from the vestibular efferent system (Goldberg and Fernandez, 1980; Highstein and Baker, 1985). Efferents provide signals that could potentially bring about adaptive rescaling (Highstein and Baker, 1985; Boyle and Highstein, 1990a). Goldberg and

Fernandez (1976) suggested that the vestibular efferent system might function to reduce sensitivities to self-generated movements. In the toadfish, activation of the efferent system results in an immediate increase in resting rate and a decrease in sensitivity to ongoing rotation in a subset of primary afferents (Boyle and Highstein, 1990a). The difficulty with this explanation is that changes in sensitivity in response to rotation alone have not been reported in primary afferents. Responses of the most sensitive group of afferents saturate with increasing stimulus velocity, starting at less than 100°/s, in both the toadfish (Boyle and Highstein, 1990b) and the chinchilla (J. M. Goldberg, pers. comm.). This saturation results in some loss of signal for high-velocity stimuli, which is what would be expected in a system that does not have the capacity to rescale. Most groups of primary afferents show linear responses during rotation in the velocity range that we tested, and thorough examination of the responses of regularly and irregularly firing vestibular afferents to rotation at a broad range of velocities provided no evidence for rescaling (Fernandez and Goldberg, 1971; Goldberg et al., 1982; Hullar and Minor, 1999; Hullar et al., 2005).

Some vestibular afferents, at least in the toadfish, carry an almost-pure acceleration signal during rotation (Boyle and Highstein, 1990b). If an acceleration signal were selectively rescaled, then we would expect a decrease in the phase lead of secondary neurons with rescaling to higher velocities (and accelerations). However, an increase in phase lead was seen instead. Changing the rotation frequency, which also varied acceleration, did not cause rescaling. We conclude that the present data are not consistent with selective changes in the acceleration signals carried by secondary neurons during adaptive rescaling, but would be consistent with selective changes in other signals, such as head or eye velocity.

3.3. *The role of adaptive rescaling in the VOR*

After recovery from UL, the VOR demonstrated a persistent saturating nonlinearity above 40°/s peak head velocity for rotation toward the damaged side. This result is consistent with earlier observations in humans, rhesus macaques and cats after UL (Maioli et al., 1983; Fetter and Zee, 1988; Tusa et al., 1996; Foster et al., 1997; Lasker et al., 2000). Saturating nonlinearities in the VOR during ipsilesional rotation were also reported after recovery from unilateral horizontal semicircular canal plugs in squirrel monkeys (Paige, 1983b; Lasker et al., 1999). We confirmed that this nonlinearity was present in the cat VOR, during 1-Hz rotation within the velocity range of adaptive rescaling in vestibular neurons.

The rescaling of neuronal sensitivities during high-velocity rotation increased the operating ranges of vestibular neurons and kept the proportion of contralesional neurons transmitting linear signals nearly constant (Fig. 7). Maintaining a linear output signal might be expected to yield strong advantages in terms of information transmission which would be reflected in VOR performance. Rescaling is present in vestibular neurons of normal cats (Melvill Jones and Milsum, 1970), but after UVD its contribution may be particularly important because the VOR encounters limits in performance. In the normal cat, nonlinear responses appear in secondary neurons but do not appear in the VOR's response, suggesting that rescaling may not be functionally important in normals. After UVD, nonlinear responses in secondary neurons persist in spite of rescaling, suggesting that rescaling may be too limited to correct the problem. This logic predicts that, in intermediate conditions, with partial loss of the vestibular signal from one side, rescaling would correct the problem and the VOR would recover completely.

In summary, we report the existence of adaptive rescaling in central vestibular neurons of alert animals after recovery from UVD. Rescaling occurs at velocities where the VOR generates saturating responses. As a result of rescaling, these neurons vary their dynamic ranges based on the range of input signals.

4. Experimental procedure

Three neutered male cats, 9–15 months old at the start of recordings, were used in this study. Before beginning experiments, cats were conditioned to sit in the apparatus with head fixed. The VOR was recorded in each cat before, and again more than 30 days after, UVD. One horizontal semicircular canal was plugged in cats C and J. In cat O, a unilateral labyrinthectomy was performed. Single unit recordings were carried out at least 60 days after UVD. Animal care guidelines of the Canadian Council of Animal Care were followed throughout.

4.1. *Surgical procedures*

Our methods for implanting head holders, search coils and guide cylinders for electrode placement have recently been described in detail (Broussard et al., 1999; Broussard et al., 2004). Briefly, cats were premedicated with Demerol, atropine and acepromazine and anesthetized with isoflurane. Buprenorphine (30 μg) was given for analgesia at the start and again at the end of surgery. A stable anesthetic plane was maintained with isoflurane (1.5–2%). Cats were positioned stereotaxically and a cylindrical steel head holder was attached to the head using dental acrylic, fixation plates and cortical screws. In the same procedure, we sutured a search coil to the sclera in one eye, in most cases the eye ipsilateral to the lesion (Broussard et al., 1999). In a second surgery, a 20-mm diameter recording cylinder (Crist Instruments) was centered, pitched 20° back from the stereotaxic vertical plane and attached to the fixation plates with dental acrylic. Buprenorphine and ketoprofen were given postoperatively for analgesia.

Our methods for canal plugging and UL were described previously (Broussard et al., 1999). Under isoflurane anesthesia, the temporal bone was carefully thinned and the middle ear opened. For the canal plug, using the long process of the incus as a landmark, a small opening was made in the horizontal semicircular canal and the lumen was tightly plugged using a piece of periosteum. For the UL, the soft tissues of the utricle, saccule and ampullae were removed. The muscle and skin were sutured closed. Postoperatively, ketoprofen was used for analgesia.

Rotation-sensitive neurons in the vestibular nuclei receive most of their excitatory input from primary afferents on the

ipsilateral side, and these tonic inputs are largely removed after UL. Canal plugs, on the other hand, do not abolish the primary afferent activity. In spite of this major difference in tonic excitatory inputs to secondary neurons, we found no difference in adaptive rescaling of vestibular neurons after HSCC plugs and after UL. Therefore data for UL and HSCC plugs are described and discussed together.

4.2. *Recording the VOR and neuronal responses*

All vestibular stimuli were sinusoidal rotations around an earth-vertical axis in complete darkness using a rate table with velocity feedback (Neurokinetics). The feedback tachometer signal was digitized as a record of head velocity. During recording, the cat sat upright in a close-fitting box, with its interaural line on the axis of rotation. A steel post, attached to the turntable superstructure, fitted inside the head holder and was bolted in place. For all VOR recordings, we positioned the head 22° nose-down from the stereotaxic plane so that the horizontal canals were near the rotation plane. For single unit recording, we positioned the horizontal semicircular canals in the plane of rotation or 30° from the plane of rotation (see below). The animal was rotated at 1 Hz and a peak velocity of 10, 20, 40, 80 and 120°/s and, in some cases, at a peak velocity of 10°/s and frequencies of 1–8 Hz.

We measured eye movements using a search coil apparatus, consisting of a phase detector (CNC Engineering) with vertical and horizontal 17″ field coils. The head was centered in both magnetic fields. We digitized vertical and horizontal eye position signals at either 1 kHz (cats J and C) or 4 kHz (cat O) using Labview software (National Instruments). Signals were digitally low-pass filtered with a cutoff of 55 Hz. Eye velocity was calculated using a 5-point differentiation algorithm. At least 60 cycles of rotation were acquired at each peak velocity. During VOR recordings, cats were kept alert by interesting noises and tactile stimuli. We did not administer amphetamine.

We recorded isolated single unit activity using glass-insulated platinum–iridium microelectrodes with impedances of 2–8 MΩ. Electrodes were positioned using a head-mounted micromanipulator (Narishige) and microdrive (Fred Haer Corp.) and driven through the dura. At intervals, the cat was anesthetized and scar tissue gently peeled away from the dura to permit the passage of microelectrodes. The medial and ventrolateral vestibular nuclei were targeted stereotaxically using recorded abducens nuclear activity as a reference point. To ensure that the cells were encoding horizontal canal signals, recordings were made while the head was tilted 22° nose-down, and then the head was repositioned 5° nose-up and more data were gathered. For type II neurons, if the cell's response increased its sensitivity with nose-up rotation, that cell was considered a vertical canal neuron and was excluded from our sample. For type I neurons, if the cell's response changed polarity during nose-up rotation, it was excluded.

A search stimulus, 1 Hz rotation at a peak velocity 10 or 20°/s, was applied while searching for cells. All of the neurons that we found had a nonzero resting discharge rate; no silent neurons were activated by the search stimulus. When a unit was isolated, trigger pulses were generated by a window discriminator (Bak Electronics). We digitized head velocity, vertical and horizontal eye position. In cats J and C spike times were recorded to the nearest 10 μs using a counter; in Cat O we digitized the trigger pulses. In both cases, the trigger pulses were used to calculate spike density (see below). In cat O we also digitized the extracellular voltage at a sample rate of 60 kHz.

Neuronal responses were recorded during rotation in darkness at 1 Hz and peak velocities of 10, 20, 40, 80 and 120°/s; isolation was frequently lost at 120°/s and those data were discarded. For each peak velocity, rotation was continuous; the table was stationary for 5–10 s between velocities while data were saved on the disk. Generally, the peak velocities were presented in increasing order but in some cases, the 20°/s file was acquired first. Finally, rotation at 10°/s was repeated in the nose-up position. The responses of most cells were recorded during periods of steady fixation in the light as the cat shifted its gaze around the recording room. These files were used to determine eye position sensitivity. In about 50% of cases the cell's resting discharge was recorded while stationary in darkness before rotation for comparison with the mean spike densities during, and the resting rates after, rotation.

4.3. *Histology*

At the end of experiments, electrolytic marking lesions were made at one recording site on each side of the brainstem by applying 5 μA of direct current for 10 min. At least 4 days after the lesion, the cat was sedated with 20 mg/kg ketamine i.m., deeply anesthetized (sodium pentobarbital, 100 mg/kg i.v.) and perfused transcardially with physiological saline followed by 10% buffered formalin. Brains were processed for histology using a freezing microtome or vibratome and stained with cresyl violet. Based on the marking lesions, the recording sites of all neurons were found to be either in the medial or the ventral lateral vestibular nucleus.

4.4. *Data analysis*

For the VOR, we averaged at least 320 cycles of head and eye velocity, from 8 days of recording, at each peak velocity. Quick phases were manually removed from the eye velocity traces prior to averaging. Ipsi- and contralesional half-cycles of rotation were analyzed separately as previously described (Broussard et al., 1999).

For the single unit recordings, we calculated spike densities by convolving the pulse trains with a Gaussian probability density function having a standard deviation of 15% of each cycle (for details see Broussard et al., 2004). At each velocity, the first cycle was discarded to eliminate mechanical transients, and the next 10 to 30 cycles were averaged. If triggering was lost during a cycle, that cycle was excluded. Cells that provided fewer than 10 acceptable cycles of data at any velocity were excluded from further analysis.

Based on their response patterns, cells were classified as type I, type II or type III. To arrive at an unambiguous classification for each frequency, we limited the response phase to within 90° of head velocity. Type I neurons increased their firing rate for ipsilateral rotation and type II neurons increased their firing rate for contralateral rotation. Type III

neurons increased their discharge rates for both directions of rotation, such that the smaller response was at least 50% of the larger one.

Type I and II cells were further classified as either eye movement (EM) or vestibular-only (V-only), as recently described (Broussard et al., 2004). Briefly, eye position sensitivity was determined by linear regression, either during steady fixation at different eye positions in the light, or at the zero-crossings of head velocity during the VOR in darkness (Broussard et al., 2004). This analysis was carried out only on data files which contained 10 or more saccades. Eight cells were excluded from eye position analysis because too few saccades were made. Among those analyzed, neurons with sensitivities to horizontal eye position of 0.5 sp/s per degree or more were classified as EM cells; others were classified as V-only.

4.5. *Sensitivity and breakpoint*

To measure the sensitivity and breakpoint of neuronal responses, spike density was plotted against head velocity (see Fig. 1). Two lines were fit to the data and the position of their intersection was adjusted along the *x*-axis to minimize the combined MSE. The spike density trace was shifted temporally to remove any phase lead or lag and optimize the fit. If the confidence intervals about the slopes were non-overlapping, a breakpoint was defined as the head velocity at the intersection of the fitted lines (as in the cutoff and saturating responses of Fig. 1). If the slopes of the two lines were not significantly different, then the response was said to be linear (Fig. 1C).

Given the nonlinear responses of many cells, consistent determination of sensitivity required set criteria for the region of the function that we chose to measure. For cutoff responses, the sensitivity was the slope of the response function that included the cell's on-direction, i.e., above the breakpoint (arrow in Fig. 1). For saturation-type responses, the sensitivity was the slope below the breakpoint (Fig. 1). In a few cases the breakpoint lay within one-quarter cycle of the peak velocity, and the central region of the function was used in determining sensitivity in those cases. After calculating sensitivity, we applied a post hoc criterion for response sensitivity, i.e., cells were included in this report only if the ratio of the mean standard error of the linear fit to the slope of the fitted line (in spikes/s per degree/s) was less than 5 for at least one of the peak rotational velocities that were tested.

Zero-velocity spike density ($SD_{H=0}$) was the spike density at 0°/s head velocity after the phase adjustment and was also used as an estimate of the resting rate. This was justified by our observation that the average $SD_{H=0}$ values for responses during rotation with a peak velocity of 10°/s were not different from the average resting rate recorded while stationary in the dark, immediately before the start of rotation. This was true for both type I or type II cells in cat O ($P > 0.5$, paired Student's *t*-test; see Fig. 5). Pre-rotation data were not gathered in cats J and C.

Individual comparisons between sensitivities and resting rates at different peak velocities were done using Student's paired *t*-tests (small sample methods), so that we could determine which absolute values of rotational velocity resulted in significant changes.

Acknowledgments

We thank Y.-F. Tan, H. Titley and H. Xiao for technical assistance and M. Wojtowicz for the use of the vibratome. This research was funded by the Canadian Institutes of Health Research. R. Heskin-Sweezie was supported by a Vision Science Research Program Fellowship and an Ontario Graduate Scholarship in Science and Technology. K. Farrow was supported by a Unilever-Lipton Graduate Scholarship.

REFERENCES

Blanks, R.H.I., Estes, M.S., Markham, C.H., 1975. Physiologic characteristics of vestibular first-order canal neurons in the cat: II. Response to constant angular acceleration. J. Neurophysiol. 38, 225–229.

Borst, A., Flanagin, V.L., Sompolinsky, H., 2005. Adaptation without parameter change: dynamic gain control in motion detection. PNAS 102, 6172–6176.

Boyle, R., Highstein, S.M., 1990a. Efferent vestibular system in the toadfish: action upon horizontal semicircular canal afferents. J. Neurosci. 10, 1570–1582.

Boyle, R., Highstein, S.M., 1990b. Resting discharge and response dynamics of horizontal semicircular canal afferents of the toadfish, *Opsanus tau*. J. Neurosci. 10, 1557–1569.

Brenner, N., Bialek, W., de Ruyter von Steveninck, R., 2000. Adaptive rescaling maximizes information transmission. Neuron 26, 695–702.

Broussard, D.M., Bhatia, J.K., Jones, G.E.G., 1999. The dynamics of the vestibulo-ocular reflex after peripheral vestibular damage: I. Frequency-dependent asymmetry. Exp. Brain Res. 125, 353–364.

Broussard, D.M., Priesol, A.J., Tan, Y.-F., 2004. Asymmetric responses to rotation at high frequencies in central vestibular neurons of the alert cat. Brain Res. 1005, 137–153.

Chen-Huang, C., McCrea, R.A., 1999. Effects of viewing distance on the responses of horizontal canal-related secondary vestibular neurons during angular head rotation. J. Neurophysiol. 81, 2517–2537.

Dean, I., Harper, N.S., McAlpine, D., 2005. Neural population coding of sound level adapts to stimulus statistics. Nat. Neurosci. 8, 1684–1689.

Dickman, J.D., Correia, M.J., 1989. Responses of pigeon horizontal semicircular canal afferent fibers. I. Step, trapezoid, and low-frequency sinusoid mechanical and rotational stimulation. J. Neurophysiol. 62, 1090–1101.

Escudero, M., de la Cruz, R.R., Delgado-Garcia, J.M., 1992. A physiological study of vestibular and prepositus hypoglossi neurones projecting to the abducens nucleus in the alert cat. J. Physiol. 458, 539–560.

Fairhall, A.L., Lewen, G.D., Bialek, W., de Ruyter von Steveninck, R.R., 2001. Efficiency and ambiguity in an adaptive neural code. Nature 412, 787–792.

Fernandez, C., Goldberg, J.M., 1971. Physiology of peripheral neurons innervating semicircular canals of the squirrel monkey: II. Response to sinusoidal stimulation and dynamics of peripheral vestibular systems. J. Neurophysiol. 34, 661–675.

Fetter, M., Zee, D.S., 1988. Recovery from unilateral labyrinthectomy in rhesus monkey. J. Neurophysiol. 59, 370–393.

Foster, C.A., Demer, J.L., Morrow, M.J., Baloh, R.W., 1997. Deficits of gaze stability in multiple axes following unilateral vestibular lesions. Exp. Brain Res. 116, 501–509.

Goldberg, J.M., Fernandez, C., 1976. The vestibular system.

Handbook of Physiology—The Nervous System, vol. III, pp. 977–1021.
Goldberg, J.M., Fernandez, C., 1980. Efferent vestibular system in the squirrel monkey: anatomical location and influence on afferent activity. J. Neurophysiol. 43, 986–1025.
Goldberg, J.M., Fernandez, C., Smith, C.E., 1982. Responses of vestibular-nerve afferents in the squirrel monkey to externally applied galvanic currents. Brain Res. 252, 156–160.
Highstein, S.M., Baker, R., 1985. Action of the efferent vestibular system on primary afferents in the toadfish, *Opsanus tau*. J. Neurophysiol. 54, 370–384.
Hullar, T.E., Minor, L.M., 1999. High-frequency dynamics of regularly discharging canal afferents provide a linear signal for angular vestibuloocular reflexes. J. Neurophysiol. 82, 2000–2005.
Hullar, T.E., Della Santina, C.C., Hirvonen, T., Lasker, D.M., Carey, J.P., Minor, L.B., 2005. Responses of irregularly discharging chinchilla semicircular canal vestibular-nerve afferents during high-frequency head rotations. J. Neurophysiol. 93, 2777–2786.
Ibbotson, M.R., 2005. Contrast and temporal frequency-related adaptation in the pretectal nucleus of the optic tracts. J. Neurophysiol. 94, 136–146.
Khatri, V., Hartings, J.A., Simons, D.J., 2004. Adaptation in thalamic barreloid and cortical barrel neurons to periodic whisker deflections varying in frequency and velocity. J. Neurophysiol. 92, 3244–3254.
Kim, K.J., Rieke, F., 2001. Temporal contrast adaptation in the input and output signals of salamander retinal ganglion cells. J. Neurosci. 21, 287–299.
Lasker, D.M., Backous, D.D., Lysakowski, A., Davis, G.L., Minor, L.B., 1999. Horizontal vestibuloocular reflex evoked by high-acceleration rotations in the squirrel monkey: II. Responses after canal plugging. J. Neurophysiol. 82, 1271–1285.
Lasker, D.M., Hullar, T.E., Minor, L.B., 2000. Horizontal vestibuloocular reflex evoked by high-acceleration rotations in the squirrel monkey: III. Responses after labyrinthectomy. J. Neurophysiol. 83, 2482–2496.
Leung, Y.Y., Bensmaia, S.J., Hsaio, S.S., Johnson, K.O., 2005. Time-course of vibratory adaptation and recovery in cutaneous mechanoreceptive afferents. J. Neurophysiol. 94, 3037–3045.
Maioli, C., Precht, W., Reid, S., 1983. Short- and long-term modifications of vestibuloocular response dynamics following unilateral vestibular nerve lesions in the cat. Exp. Brain Res. 50, 259.
McLaughlin, S.C., 1967. Parametric adjustment in saccadic eye movements. Percept. Psychophys. 2, 259–362.
Melvill Jones, G., Milsum, J.H., 1970. Characteristics of neural transmission from the semicircular canal to the vestibular nuclei of cats. J. Physiol. 209, 295–316.
Melvill Jones, G., Milsum, J., 1971. Frequency-response analysis of central vestibular unit activity resulting from rotational stimulation of the semi-circular canals. J. Physiol. 219, 191–215.
Nagel, K.I., Doupe, A.J., 2006. Temporal processing and adaptation in the songbird auditory forebrain. Neuron 51, 845–849.
Newlands, S.D., Perachio, A.A., 1990a. Compensation of horizontal canal related activity in the medial vestibular nucleus following unilateral labyrinth ablation in the decerebrate gerbil: I. Type I neurons. Exp. Brain Res. 82, 359–372.
Newlands, S.D., Perachio, A.A., 1990b. Compensation of horizontal canal related activity in the medial vestibular nucleus following unilateral labyrinth ablation in the decerebrate gerbil: II. Type II neurons. Exp. Brain Res. 82, 373–383.
Ohzawa, I., Sclar, G., Freeman, R.D., 1985. Contrast gain control in the cat's visual system. J. Neurophysiol. 54, 651–667.
Paige, G.D., 1983a. Vestibuloocular reflex and its interactions with visual following mechanisms in the squirrel monkey: I. Response characteristics in normal animals. J. Neurophysiol. 49, 134–168.
Paige, G.D., 1983b. Vestibuloocular reflex and its interactions with visual following mechanisms in the squirrel monkey: II. Response characteristics and plasticity following unilateral inactivation of horizontal canal. J. Neurophysiol. 49, 152–168.
Rabbitt, R.D., Boyle, R., Holstein, G.R., Hightstein, S.M., 2005. Hair-cell versus afferent adaptation in the semicircular canals. J. Neurophysiol. 93, 424–436.
Schwartz, O., Simoncelli, E.P., 2001. Natural signal statistics and sensory gain control. Nat. Neurosci. 4, 819–825.
Shimazu, H., Precht, W., 1966. Inhibition of central vestibular neurons from the contralateral labyrinth and its mediating pathway. J. Neurophysiol. 29, 467–492.
Smith, P.F., Curthoys, I.S., 1988a. Neuronal activity in the contralateral medial vestibular nucleus of the guinea pig following unilateral labyrinthectomy. Brain Res. 444, 295–307.
Smith, P.F., Curthoys, I.S., 1988b. Neuronal activity in the ipsilateral medial vestibular nucleus of the guinea pig following unilateral labyrinthectomy. Brain Res. 444, 308–319.
Tusa, R.J., Grant, M.P., Buettner, U.W., Herdman, S.J., Zee, D.S., 1996. The contribution of the vertical semicircular canals to high-velocity horizontal vestibulo-ocular reflex (VOR) in normal subjects and patients with unilateral nerve section. Acta Otolaryngol. 116, 507–512.